



Research papers

Temporal downscaling rainfall and streamflow records through a deterministic fractal geometric approach



Mahesh L. Maskey^a, Carlos E. Puente^{a,*}, Bellie Sivakumar^{a,b,c,d}

^a Department of Land, Air & Water Resources, University of California, Davis, CA 95616, USA

^b UNSW Water Research Centre, School of Civil and Environmental Engineering, The University of New South Wales, Sydney, NSW 2052, Australia

^c Department of Civil Engineering, Indian Institute of Technology Bombay, Powai, Mumbai, Maharashtra 400 076, India

^d State Key Laboratory of Hydrosience and Engineering, Tsinghua University, Beijing 100 084, China

ARTICLE INFO

Keywords:

Disaggregation
Fractal-multifractal
Deterministic
Rainfall
Streamflow

ABSTRACT

A deterministic geometric approach, the fractal-multifractal (FM) method, is proposed to temporally downscale (disaggregate) rainfall and streamflow records. The applicability of the FM approach is tested on: (1) two sets of rainfall records—one from Laikakota, Bolivia and the other from Tinkham, Washington, USA; and (2) two distinct sets of streamflow records—for water years 2005 and 2008 from the Sacramento River, California, USA. For the purpose of validation, the available daily records are first aggregated into weekly, biweekly, and monthly records and then the FM method is applied to downscale such sets back into the daily scale. The results indicate that the FM method, coupled with a threshold to capture the high intermittency of rainfall and a smoothing parameter to get the milder texture of streamflow, readily generates daily series (over a year) based on weekly, biweekly, and monthly accumulated information, which reasonably preserves the time evolution of the records (especially for streamflow) and captures a variety of key statistical attributes (e.g., autocorrelation, histogram, and entropy). It is argued that the FM deterministic downscalings may enhance and/or supplement available stochastic disaggregation methods.

1. Introduction

The general lack of high-resolution hydrologic information (both in time and in space) limits our ability in the proper design, simulation, and operation of many water resources infrastructures, such as those associated with flood control and urban drainage. A common practice to overcome this problem is to disaggregate/downscale information available at a coarse scale into finer scales through some downscaling techniques. Such disaggregation approaches are generally designed to preserve some basic statistical characteristics of the records, including low-order moments, autocorrelations, power spectra, and multifractal properties, among others.

A large number of temporal disaggregation approaches and models exist in the literature. Very early disaggregation models were generally based on statistical notions (e.g., Pattison, 1965; Grace and Eagleson, 1966; Bras and Rodriguez-Iturbe, 1976) that preserve suitable moments. Some key contributions in this area are as follows. Valencia and Schaake (1972, 1973) introduced a linear disaggregation model, aimed at the preservation of low-order moments at various scales – yearly, monthly, and daily. However, this model does not account for the

rather skewed distributions and highly intermittent character of rainfall. Subsequently, Mejia and Roussellee (1976), Tao and Delleur (1976), Hoshi and Burges (1979), Todini (1980), Stedinger and Vogel (1984), Hershenhorn and Woolhiser (1987), and Connolly et al. (1998), among others, popularized such a linear disaggregation model, with important modifications to the underlying notions and implementation procedures. Despite the improvements in these models and their applications, limitations in such approaches continue to be highlighted. For instance, this class of models, in truth, belongs to a class of parametric techniques that requires prior assumptions about the probability distributions of the model parameters (e.g., Alvisi et al., 2015).

Looking for an improved approach, Koutsoyiannis and Xanthopoulos (1990) introduced a single-site dynamic disaggregation model as a step-wise procedure, which accounts for low-level variables, to combine rainfall model with Markovian structures and normal or gamma distributions. Employing such a model, Koutsoyiannis (1992) converted a sequential simulation model into a disaggregation model, so that the output could explicitly preserve second order statistics of low-level variables at the finer time scale. Later on, Koutsoyiannis (1994) noted that these models are not applicable for short-scale

* Corresponding author.

E-mail address: cepunte@ucdavis.edu (C.E. Puente).

List of Acronyms

$X_\tau(t_\tau)$	observed records at scale τ	MEA_C	maximum error in accumulated sets at coarse scale
$\widehat{X}_\tau(t_\tau)$	FM fitted set at scale τ	$NSED_C$	Nash-Sutcliffe efficiency for data at coarse scale
$AX_\tau(t_\tau)$	observed accumulated records at scale τ	REA_F	root mean square error in accumulated record at fine (daily) scale
$\widehat{AX}_\tau(t_\tau)$	FM fitted accumulated set at scale τ	MEA_F	maximum error in accumulated record at fine (daily) scale
$R_\tau(t_\tau)$	observed rainfall at scale τ	$NSED_F$	Nash-Sutcliffe efficiency for data at fine (daily) scale
$AR_\tau(t_\tau)$	observed accumulated rainfall at scale τ	$NSEA$	Nash-Sutcliffe efficiency for autocorrelation
$Q_\tau(t_\tau)$	observed streamflow at scale τ	$NSEH$	Nash-Sutcliffe efficiency for histogram
$AQ_\tau(t_\tau)$	observed accumulated streamflow at scale τ	$NSEE$	Nash-Sutcliffe efficiency for entropy
$RMSEA_\tau$	root mean square error in accumulated sets at scale τ	NZ	number of zeros in a rainfall set
$MAXEA_\tau$	maximum error in accumulated sets at scale τ	$PD90$	percent histogram mass in FM fitted records corresponding to 90% in observed data
REA_C	root mean square error in accumulated sets at coarse scale		

rainfall disaggregation, but that they could be improved by making use of properties of gamma distributions. He also suggested the possibility to link them with a Markovian structure relying on only three parameters, and that this notion could be used to solve the engineering problems that seek defining a design storm. However, Zarris et al. (1998) argued that such an approach, defined for flood frequency curves, may not be adequate for continuous sets.

In light of the fact that natural records, as measured around the world and commonly used in scientific investigations, are rather complex and intricate, the late great mathematician Benoit Mandelbrot suggested that geophysical records could exhibit a form of statistical self-similarity, that possibly bridges various temporal and spatial scales, via a concept now known as multifractality (Mandelbrot, 1982, 1989). Following such a lead, a number of studies have implemented stochastic (fractal, multifractal) theories in order to deal with the erratic and intermittent patterns of rainfall, streamflow, and other geophysical sets at hand; see, for example, Gupta and Waymire (1990), Tessier et al. (1993), and Lovejoy and Schertzer (2013), among others. Using these notions, Olsson (1998) evaluated the possibility of modeling and disaggregating temporal rainfall using a multiplicative cascade model, which had the ability to preserve the scaling behavior of the records. This model was subsequently tested by Olsson and Berndtsson (1998), who showed that the model may account for seasonal non-stationarities. Such was also considered by Güntner et al. (2001), who, by studying issues regarding the transferability of parameters, identified the reasons why the autocorrelation function may be underestimated and why the model may overestimate extreme events.

While classical and multifractal stochastic disaggregation models produce reasonable realizations of rainfall and streamflow processes, other approaches have also been tried searching for “better” outcomes. For instance, Lall (1995) proposed a nonparametric procedure that captures the nonlinearities present in the records, and Kumar et al. (2000) employed such a method to disaggregate daily streamflow and to approximate the probability distribution of a disaggregated streamflow vector at multiple sites. Based on such nonparametric notions, Prairie et al. (2007) proposed a technique for space-time disaggregation of streamflow, which ended up stressing that the nonlinear character of streamflow (and other hydrologic processes) cannot be disaggregated using traditional techniques, due to a high-dimensionality problem.

Continuing with alternative approaches and in recognition of the presence of chaotic behavior in geophysical processes (e.g., Lorenz, 1963) and in their transformation between different scales, Sivakumar (2001) explored the presence of chaos in rainfall time series observed at four different temporal scales in the Leaf River basin, Mississippi, USA, using phase space reconstruction and correlation dimension. The outcomes of such a study led Sivakumar et al. (2001) to investigate the possibility of using chaos theory to transform rainfall from one scale to another. Analyzing the dimensionality of the weights of the rainfall distribution between (any) two scales using the correlation dimension method and identifying the presence of chaotic behavior in such

weights, Sivakumar et al. (2001) also proposed a chaotic model for rainfall disaggregation based on an approach that uses local approximation in the reconstructed phase space. Sivakumar et al. (2004) subsequently employed this approach to disaggregate streamflow in the Mississippi River basin at St. Louis, Missouri, USA. Despite the encouraging outcomes from chaos theory-based studies in hydrology, some criticisms of such studies have been raised; see Schertzer et al. (2002) and Sivakumar et al. (2002) for a discussion. A comprehensive account of the applications of chaos theory in hydrology, including for rainfall and streamflow disaggregation, is presented in Sivakumar (2017).

On a systematic practical setting, Lanza et al. (2001) reviewed several works on rainfall downscaling techniques and pointed out that direct validation of downscaling approaches is problematic due to a lack of reliable measurements. Pointing out that the absence of high-resolution rainfall records clearly introduces uncertainties in the rainfall-runoff processes involved, they emphasized the need to conduct standard synthetic tests in order to fully compare the different approaches. Koutsoyiannis (2003) and Koutsoyiannis et al. (2003) provided a general overview of the development of rainfall disaggregation models, most of which generate synthetic time series for partial durations.

Recently, an “ensemble downscaling” method has been proposed by combining different sources of information. For instance, Liu et al. (2016) introduced an approach that couples a Bayesian model and ensembles from three statistical downscaling methods, to provide a scientific basis for the study of runoff response to climate change: one based on a support vector machine aimed at capturing nonlinear regression relationships between variables, another on a weather generator scheme to yield long time series as needed in the risk analysis of climate change, and a third based on statistical downscaling model as a decision support tool. Such a study demonstrated the better performance of the “ensemble downscaling” method based on Bayesian model averaging than a single statistical downscaling approach.

The downscaling techniques summarized above could be based on either stochastic or dynamical models. However, either type of models has its own limitations. Stochastic techniques (e.g., regression models, weather generators) are based on simplified assumptions, require substantially long records and large number of parameters, and are seldom capable of preserving the finer details present in hydrologic records. Dynamical techniques, on the other hand, turn out to be computationally intensive; see Fowler et al. (2007) for details, especially in the context of downscaling approaches, in time and space, for global climate model outputs.

To deal with the intricacies inherent in natural records, Puente (1996) had earlier introduced the notion that a given “seemingly-random” set could be represented as a fractal transformation of a multifractal measure. As a consequence, a procedure—named the fractal-multifractal (FM) method—was introduced, which, besides being assigned a physical interpretation (Cortis et al., 2013), (a) is

capable of producing a vast class of patterns defined over one and higher dimensions that look like natural sets; and (b) gives sets that may be conditioned to capture the overall trends and inherent details present on available records, beyond the preservation of some relevant statistical attributes, such as moments, autocorrelation function, power spectrum, and multifractal spectrum. Upon its discovery, the FM method has been found useful in various applications that include, among others: (a) the encoding of various rainfall events lasting a few hours (e.g., Puente and Obregón, 1996; Cortis et al., 2009, 2013; Huang et al., 2013); (b) the modeling of spatial contamination patterns in groundwater (Puente et al., 2001a,b); (c) the encoding of daily precipitation (Maskey et al., 2016a; Puente et al., 2018); (d) the encoding of streamflow gathered daily over a year (Maskey et al., 2016b); and (e) the simulation of daily rainfall (Maskey et al., 2016c) and of daily streamflow (Maskey et al., 2017).

The encouraging outcomes from these applications suggest the possibility of using the FM approach also for temporal downscaling of hydrologic data. Herein, we propose an FM approach for downscaling rainfall and streamflow records. We validate the approach: (1) on rainfall using one year of data each from Laikakota, Bolivia and Tinkham, Washington State, USA; and (2) on streamflow employing two different years of data from the Sacramento River, California, USA. Having available daily records at such sites, we first aggregate such data to weekly, biweekly, and monthly scales and then use the FM method to disaggregate to daily scale to compare with the original records.

The rest of this article is organized as follows. Section 2 re-visits the original fractal-multifractal approach and presents adaptations used here to encode both rainfall and streamflow sets. Section 3 explains how the FM method is used in order to define specific downscales. Section 4 presents the results and discussion for the obtained disaggregated patterns for rainfall and Section 5 reports such for streamflow. Section 6 summarizes the findings and provides remarks for further research.

2. The fractal multifractal method and adaptations for rainfall and streamflow

According to the FM framework, geophysical records may be represented, geometrically and in a system-theoretic sense, as “outputs” (derived distributions) produced by a complex “system” (defined by a fractal interpolating function) when the “inputs” to the system are also complex (multifractal measures) (Puente, 1996). This section briefly explains the FM approach and provides adaptations of the original notions that allow the method to be used to represent highly-intermittent records (e.g., daily rainfall sets) and mildly-intermittent records (e.g., daily streamflow sets).

2.1. Theoretical framework

Following Barnsley (1988), a fractal interpolating function f , defined from x into y (i.e., $f: x \rightarrow y$) and passing through $N + 1$ pre-specified points (x_n, y_n) satisfying $x_0 < x_1 < \dots < x_N$, is obtained iterating N simple affine maps, from the plane to the plane, i.e., from (x, y) to (x, y) , of the special form:

$$w_n \begin{pmatrix} x \\ y \end{pmatrix} = \begin{pmatrix} a_n & 0 \\ c_n & d_n \end{pmatrix} \begin{pmatrix} x \\ y \end{pmatrix} + \begin{pmatrix} e_n \\ f_n \end{pmatrix} \quad n = 1, \dots, N. \tag{1}$$

When these maps are constrained so that they contract the space in x :

$$w_n \begin{pmatrix} x_0 \\ y_0 \end{pmatrix} = \begin{pmatrix} x_{n-1} \\ y_{n-1} \end{pmatrix}, \quad w_n \begin{pmatrix} x_N \\ y_N \end{pmatrix} = \begin{pmatrix} x_n \\ y_n \end{pmatrix} \tag{2}$$

i.e., so that the n^{th} map compresses the first and last interpolating points into inner interpolating points. When the parameters d_n are less than one in magnitude, the iterations of such maps w_n indeed define point by point the graph G of a function f , i.e., $G = \{(x, f(x)) | x \in [x_0, x_N]\}$. By

doing so, a set becomes the unique “fixed-point” of the maps w_n , as successive calculations of images already in G , in any order, remain in the same graph, i.e., $G = \bigcup_{n=1}^N w_n(G)$.

The conditions defined in Eq. (2) yield simple systems of linear equations that allow finding the coefficients a_n, c_n, e_n and f_n , in terms of the coordinates by which the fractal interpolating function passes, i.e., (x_n, y_n) , and also the parameters d_n , which, given their usage in Eq. (1), are also known as vertical scalings (Barnsley, 1988). At the end, specifying the interpolating points and the scaling parameters allows defining, via iterations, a convoluted function f whose graph has a fractal dimension $D \in [1, 2)$, and hence its notation.

In a practical setting, the graph of such a function f may be found, indeed point by point, iterating in any order the affine maps w_n , ultimately sampling the unique “attractor” G following a procedure known in the literature as the “chaos game” (Barnsley, 1988). Such a process starts at a point within G (say, an interpolating point) and progresses as per arbitrary “coin tosses” or iterating proportions assigned to the N maps. After enough iterations, the process not only converges to the graph of a function f but also induces a unique invariant measure (a distribution) over G as well. The latter, when projected over the x and y coordinates, yields interesting histograms that typically exhibit non-trivial intermittenencies and possesses multifractal properties. These sets turn out to be inherent to the calculations and may be displayed at arbitrary scales just by varying the size and number of bins used to get the histograms. While the natural projection over x is a deterministic multinomial multifractal measure dx generated via a multiplicative cascade (e.g., Mandelbrot, 1989; Puente, 1996), the projections dy over y are deterministic derived distributions of dx via a fractal function f , which typically resemble complex natural patterns (Puente 1996, 2004).

These notions turn out to be akin to a generalization of the description of turbulent dissipation as a random binomial multifractal (Meneveau and Sreenivasan, 1987) and also to the construction of other intermittent sets as random realizations of Levy processes from universal multifractals (Lovejoy and Schertzer, 2013). As mentioned earlier, the outcomes produced by the fractal-multifractal method could also be interpreted physically, as specific realizations of a non-trivial multiplicative cascade process, in a way that a generic derived measure dy represents a suitable geometric entity to represent natural phenomena (Cortis et al., 2013).

These abstract ideas are further illustrated next as used to represent both highly-intermittent rainfall sets and mildly-intermittent streamflow series. So that the reader may better follow the notions, the next sections will be based on specific numerical examples.

2.2. FM representation of rainfall sets

Fig. 1 illustrates how the FM notions may be used to model highly intermittent sets. As shown, there is a fractal function f_1 passing through the four interpolating points $\{(0, 0), (0.28, 1.12), (0.78, -2.62), (1, 1)\}$ (shown as filled circles) and induced via the iteration of the three maps:

$$w_1 \begin{pmatrix} x \\ y \end{pmatrix} = \begin{pmatrix} 0.28 & 0 \\ 1.75 & -0.63 \end{pmatrix} \begin{pmatrix} x \\ y \end{pmatrix} \tag{3}$$

$$w_2 \begin{pmatrix} x \\ y \end{pmatrix} = \begin{pmatrix} 0.50 & 0 \\ -3.89 & 0.14 \end{pmatrix} \begin{pmatrix} x \\ y \end{pmatrix} + \begin{pmatrix} 0.28 \\ 0.78 \end{pmatrix} \tag{4}$$

$$w_3 \begin{pmatrix} x \\ y \end{pmatrix} = \begin{pmatrix} 0.22 & 0 \\ 3.63 & 0.27 \end{pmatrix} \begin{pmatrix} x \\ y \end{pmatrix} + \begin{pmatrix} 1.12 \\ -2.63 \end{pmatrix}, \tag{5}$$

playing the chaos game according to proportions, in order, 52%, 2%, and 46%.

These maps, all having the structure of Eq. (1) and with coefficients defined while satisfying the contracting conditions in Eq. (2), have vertical scalings $d_1 = -0.63, d_2 = 0.14$, and $d_3 = 0.27$, and transform the domain $[0, 1]$ in x into the sub-intervals, in order, $[0, 0.28], [0.28, 0.78]$, and $[0.78, 1]$. As shown in the figure, the iterations induce, in addition to the fractal function f_1 (whose graph G_1 has a low fractal dimension of

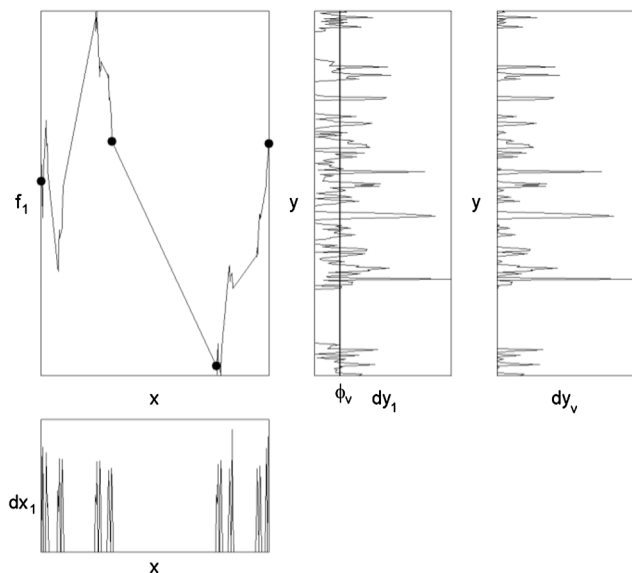


Fig. 1. The FM approach for highly-intermittent records: from a multifractal x vs. dx_1 to a derived projection y vs. dy_1 , via a fractal interpolating function $f_1: x \rightarrow y$. The set y vs. dy_v is a pruned version of dy_1 below a threshold ϕ_v in order to define further intermittency.

1.03), projected histograms dx_1 and ddy_1 , of obtained values over x and y , respectively, which may be obtained at an arbitrary resolution, just by having a suitable number of bins over which chaos game numerical calculations are grouped—273 bins for this particular example. While dx_1 (the horizontal “input”) (i.e., x vs. dx_1) is a deterministic multinomial multifractal having almost a zero value in the middle due to the 2% weight assigned to map w_2 , dy_1 (the “output” plotted vertically) (i.e., y vs. dy_1) is a deterministic derived measure, i.e., $dy_1 = f_1^{-1}(dx_1)$, in which a dy_1 value (at a given level y) is the sum of all “events” over x corresponding to such a level. The object dy_1 , akin to a distribution, can therefore be explained as a transformation of a multiplicative cascade, yielding, in this example, a highly-intermittent set that resembles rainfall records gathered daily, when y denotes time and dy_1 rainfall intensity.

Fig. 1 also includes (on the right) a set that results from an adaptation of the method, which yields other derived sets that may be used to further approximate rainfall records containing yet additional intermittency and many more zeroes. Such an object, named dy_v to acknowledge a vertical cutoff (i.e., in the y -coordinate), is naturally found from dy_1 by discarding “traces” below a threshold ϕ_v , as marked in the center plot. This new set, shown re-normalized so that it integrates to one as dy_1 , may be adjusted so that it better preserves natural records (Maskey et al., 2016a, 2016c).

2.3. FM representation of streamflow sets

Fig. 2 depicts the construction of a mildly-intermittent derived distribution. As before, another fractal function f_2 , passing through the four interpolating points marked $\{(0, 0), (0.27, -4.72), (0.91, -2.40), (1, 1)\}$, is defined via the iteration of the three maps, and distinct from those used earlier, given by:

$$w_1 \begin{pmatrix} x \\ y \end{pmatrix} = \begin{pmatrix} 0.27 & 0 \\ -5.24 & 0.52 \end{pmatrix} \begin{pmatrix} x \\ y \end{pmatrix} \tag{6}$$

$$w_2 \begin{pmatrix} x \\ y \end{pmatrix} = \begin{pmatrix} 0.64 & 0 \\ 2.63 & -0.31 \end{pmatrix} \begin{pmatrix} x \\ y \end{pmatrix} + \begin{pmatrix} 0.27 \\ -4.72 \end{pmatrix} \tag{7}$$

$$w_3 \begin{pmatrix} x \\ y \end{pmatrix} = \begin{pmatrix} 0.09 & 0 \\ 4.28 & -0.87 \end{pmatrix} \begin{pmatrix} x \\ y \end{pmatrix} + \begin{pmatrix} 0.91 \\ -2.4 \end{pmatrix}, \tag{8}$$

used according to the proportions, in order, 24%, 44%, and 32%.

These maps, all having the simple structure of Eq. (1) and with coefficients satisfying the contracting conditions in Eq. (2), have scalings $d_1 = 0.52$, $d_2 = -0.31$, and $d_3 = -0.87$. Their iteration, according to the aforementioned proportions, result in the fractal function f_2 whose graph, as seen, requires more ink than the previous f_1 , as its graph G_2 has a larger fractal dimension of 1.33. While the shown “input” dx_2 is still a rather intermittent multinomial multifractal (no longer with close to zero values, however), the new “output” derived distribution dy_2 , computed this time over 365 bins, is smoother than dy_1 before, as the bulkier fractal function f_2 adds an increasing number of events over x , i.e., $dy_2 = f_2^{-1}(dx_2)$. As such, the deterministic histogram dy_2 (i.e., y vs. dy_2) becomes suitable for modeling mildly-intermittent records, like streamflow data gathered daily, once again with y denoting time and dy_2 discharge. Fig. 2 also includes on its rightmost plot a further adaptation for the encoding of streamflow records, which consists of finding a new object dy_s , just for appearance purposes, by performing local smoothing on the histogram dy_2 (Maskey et al., 2016b, 2017).

In practice, the modeling of a given rainfall or streamflow set requires the solution of an inverse problem over plausible FM parameters, namely: (a) the interpolating points through which a fractal interpolating function passes (here assumed without lack of generality that the first and last points are $(0,0)$ and $(1,1)$); (b) the vertical scalings d_n ; (c) the iteration frequencies associated with each map in chaos game calculations (one minus the number of maps); and (d) a vertical threshold for rainfall modeling or a smoothing parameter for streamflow calculations. Hence, the usage of fractal functions defined via three affine maps, as shall be used herein based on our previous experience, requires a total of 10 FM parameters (four interpolating coordinates, $\{(x_1, y_1), (x_2, y_2)\}$, three scalings, d_1, d_2 and d_3 , two iteration frequencies, p_1 and p_2 ($p_3 = 1 - p_1 - p_2$), and one extra parameter for the adaptation, as defined above).

3. FM temporal downscaling methodology

This section describes the approach used herein to downscale (disaggregate) a given temporal set, either rainfall or streamflow, using the FM approach. It also includes information pertaining to the evaluation of goodness of the proposed approach.

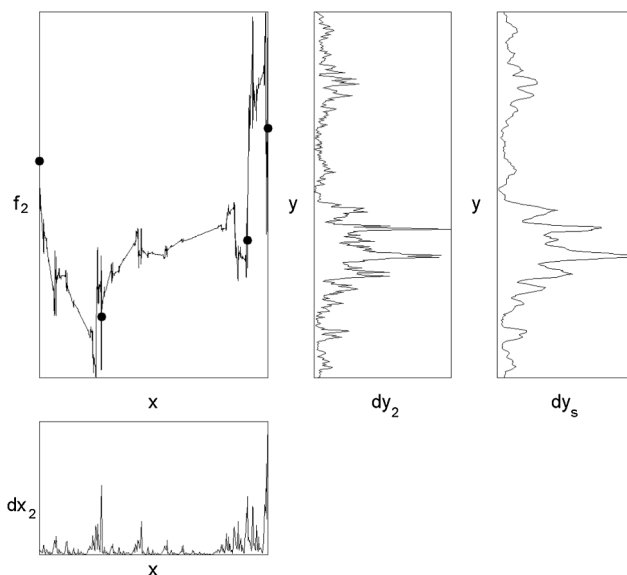


Fig. 2. The FM approach for mildly-intermittent sets: from a multifractal x vs. dx_2 to a derived projection y vs. dy_2 , via a fractal interpolating function $f_2: x \rightarrow y$. The set y vs. dy_s is an averaged version of dy_2 for further smoothness.

3.1. From coarse to fine scales

As explained in Section 1, there is a multitude of methods that may be employed to disaggregate both rainfall and streamflow records. Here, we propose, based on the success of the FM notions (Maskey et al., 2016a,b; Puente et al., 2018), an alternative geometric approach for temporal disaggregation from a coarse resolution (week, biweek, or month) to a fine resolution (day), as follows.

1. Given records (depths or volumes) at a coarse resolution, say every τ days and for a total of N periods, $X_\tau(t_\tau)$, such a set is first normalized so that it integrates to one. Then, its corresponding accumulated set (i.e., mass function), $AX_\tau(t_\tau)$, is upgraded so that $AX_\tau(1) \equiv 0$ and in such a way that $AX_\tau(M_\tau) = 1$, where $M_\tau = N + 2$.
2. With the normalized accumulated records at resolution τ , $AX_\tau(t_\tau)$, specified, such a set becomes a target for a suitable representation via the FM approach. This entails finding the “best” FM parameters, θ_τ , minimizing the square errors of the available M_τ accumulated values and following a numerical optimization approach.
3. If the calculations are performed in such a way that internal FM computations happen at the daily scale (i.e., employing precisely $N \cdot \tau$ bins in chaos game histogram calculations) while accumulating at the τ scale for optimization purposes, the implicit derived measure dy within the procedure and at the daily scale would automatically be an estimate for downscaling the normalized information at the fine scale.
4. When such a set is de-normalized by the total depth or volume for such a coarse set, a disaggregated FM representation of the geophysical process is found.

In the present study, these notions are tested for downscaling rainfall and streamflow records from resolutions of $\tau = 7$ (weekly), 14 (biweekly), and 30 days (monthly) into daily sets. Certainly, the notions could also be used in a similar fashion to obtain temporal downscales involving arbitrary scales, that is, finer than daily.

3.2. Solution strategy

The computation of fractal functions and projections associated with the FM approach happens to be a rather efficient procedure. However, as there are no analytical formulas for the derived measures, finding an FM representation for a given set requires a numerical scheme for solving an inverse optimization problem. As illustrated in Section 2, the search space when iterating three maps requires searching in 10 dimensions, but such is no obstacle for finding suitable solutions.

Based on our experience, a heuristic optimization scheme, a generalized version of the particle swarm optimization algorithm, may be used to find a close solution of an FM inverse problem (Fernández Martínez et al., 2010; Huang et al., 2013; Maskey et al., 2016a). In particular, and to circumvent the dimensionality of the search procedure, the searches for the highly-intermittent rainfall and mildly-intermittent streamflow records herein are performed as follows. While the rainfall records employ 200 randomly generated swarms made up of 500 FM parameter values, the smoother streamflow sets use 100 randomly selected swarms containing only 300 FM parameter sets. Then, all such swarms are allowed to evolve (having all members as leaders), for 300 iterations for rainfall and only 80 for streamflow. At the end, the best solution found over all swarms, even if a local optima, is considered to be the “optimal solution.” As shall be seen, the notions yield reasonable results, and finding such parameters only takes a day of computation for rainfall and 4 h for streamflow on a personal computer.

As mentioned in Section 3.1, the objective function used in the calculations is defined as in previous studies (e.g., Obregón et al.,

2002a,b; Huang et al., 2012, 2013; Maskey et al., 2016a,b). Specifically, the L^2 norm (i.e., the root mean square error) of the coarse accumulated records, every τ days, vs. the accumulated FM approximations, also every τ days, over the number of such periods over a water year, is minimized. Mathematically, such an objective function is defined as:

$$RMSEA_\tau = \sqrt{\frac{1}{M_\tau} \sum_{t=1}^{M_\tau} [AX_\tau(t_\tau) - \widehat{AX}_\tau(t_\tau)]^2} \tag{9}$$

where M_τ is the number of periods in increments of τ days, and $AX_\tau(t_\tau)$ and $\widehat{AX}_\tau(t_\tau)$ are the accumulated records and accumulated FM-related fits, as defined in Section 3.1.

Attempting to ensure that FM solutions share similar geometrical features with a target set, the aforementioned objective function is penalized so that: (a) the maximum deviations between the measured and the FM fitted records ($MAXEA_\tau$) should not exceed a value of 10% on any given period considered; and (b) the discrepancy between the length of the FM data set and that of the observed set, from beginning to end and over the periods, should be less than 5% of that of the observed set. For downscaling of rainfall, an additional penalty is imposed so that the number of zeros (no-rain events) present in the FM representation will not be more than 10% of those in the actual set.

3.3. Assessment of model performance

To validate the quality of the proposed FM approach in the context of downscaling, observed data sets at the daily scale are employed. This readily allows calculation of aggregated sets at a scale τ to be fitted by the FM method and then the performance of the disaggregation notions is validated using the original records at the finer resolution.

The performance evaluation is done in terms of various statistics, not included in the optimization exercise, and also extended to the daily FM sets. Such include the root mean square error, the maximum error in the accumulated set, and the Nash-Sutcliffe efficiency for the implied data, both at the τ coarse scale employed in the optimization (REA_C , MEA_C and $NSED_C$) and at the disaggregated daily (fine) scale (REA_F , MEA_F and $NSED_F$). Moreover, comparison (visual validation) is made by plotting the implied records at the distinct scales and by including (at the daily scale only) the autocorrelation function (ρ), histogram (H), and Rényi entropy function (E), which are further compared in terms of Nash-Sutcliffe efficiency values.

Herein, the Rényi entropy function for the daily data is defined as

$$E = \frac{1}{1-q} \log \left(\sum_{t=1}^N X(t)^q \right), \tag{10}$$

where $X(t)$ is the rainfall or streamflow (intensity or discharge) value for day t (observed or fitted), N is the number of days of activity in a year, and q is a weight that varies from -5 to 5 for streamflow and from 0.1 to 5.1 for rainfall, in order to avoid the presence of zero values.

The well-known Nash-Sutcliffe efficiency (Nash and Sutcliffe, 1970), for data sets or a given statistic, is defined in a general sense as

$$NSE = 1 - \frac{\sum_{i=1}^S (r_i - \hat{r}_i)^2}{\sum_{i=1}^S (r_i - \bar{r})^2}, \tag{11}$$

where r_i is the i th statistical value (or value) for an observed set, \bar{r} is the mean of such a statistic (or value) over the total number of statistics (values) considered (S), and \hat{r}_i is the i th statistic (fitted value) for an FM-downscaled set.

4. Downscaling of rainfall records

To establish the applicability of the FM-based downscaling approach in the context of rainfall records, 7-, 14-, and 30-day accumulated records (i.e., weekly, biweekly, and monthly scales) computed

from available daily records are analyzed at two sites: one from Laikakota, Bolivia for water year 1966 (from September 1, 1965 to May 31, 1966 and spanning 273 days) and the other from Tinkham, Washington State, USA for water year 1995 (from October 1, 1994 to September 30, 1995 and spanning the whole 365 days).

As mentioned before, rainfall data sets are normalized, so that the accumulated volume becomes a unity prior to using the FM method at all scales. As experience suggests that the inherent complexity in the daily sets may itself be achieved by the FM method employing three maps plus further trimming below a threshold (Maskey et al., 2016a), highly intermittent representations, as in Fig. 1, are employed that rely on the 10 FM parameters defined by the end of Section 2, yielding, at the daily scale, a compression ratio of 27:1 for Laikakota and 37:1 for Tinkham. Here, the parameters, including a vertical threshold, are to be obtained numerically, as explained in Section 3.2.

4.1. Rainfall set from Laikakota, Bolivia

Fig. 3 presents the implementation of the FM method to the rainfall set from Laikakota, Bolivia. The two graphs on the top right portray, respectively, the measured daily rainfall set for water year 1966 and the corresponding accumulated rainfall over the water year comprising 273 days. As may be seen, the records exhibit noticeable intermittency, contain three major peaks, and have at least six distinct regions of sustained lack of rain. The rough accumulated rain profile dips below the average slope line first, but it then crosses it and remains above it at

about four months into the season.

The next three rows in Fig. 3 present the results for 7-day, 14-day, and 30-day rainfall data. Shown in these plots are the real sets (in black) and the FM representations (in gray), including both the records and corresponding accumulated profiles. The FM fittings at the 7-, 14-, and 30-day scale are shown on the left, and the corresponding FM downscales at the daily scale are depicted on the right. An observant reader may notice that the construction of the derived measure d_{y_i} in Fig. 1, corresponds, after due flipping, to the 7-day downscale results in Fig. 3, i.e., the set shown on the third column and second row of the figure. The actual values of the FM parameters for such sets, at various disaggregation scales, are included in the first three rows of Appendix A.

As clearly seen in Fig. 3 for the accumulated rainfall plots, t_τ vs. AR_τ , all optimized FM representations fit the accumulated records at all scales reasonably well. Although the overall geometries on the first column of the graph do show some imperfections in fitting the data itself, their overall shapes follow closely the records and accumulated sets (in gray, on the second column). This implies that the penalties imposed while doing the searches, as described in Section 3.2, are satisfied. As may be verified from Table 1, the root mean square errors at a coarse resolution obtained for the accumulated sets ($REAC$) are certainly rather small, as they are, in order, 3.1, 2.8, and 3.1%, for FM representations at the 7-, 14-, and 30-day scales. The goodness of the fits may also be seen in the magnitude of the maximum errors in accumulated sets ($MEAC$), which are, for increasing scales, 8.7, 6.0, and

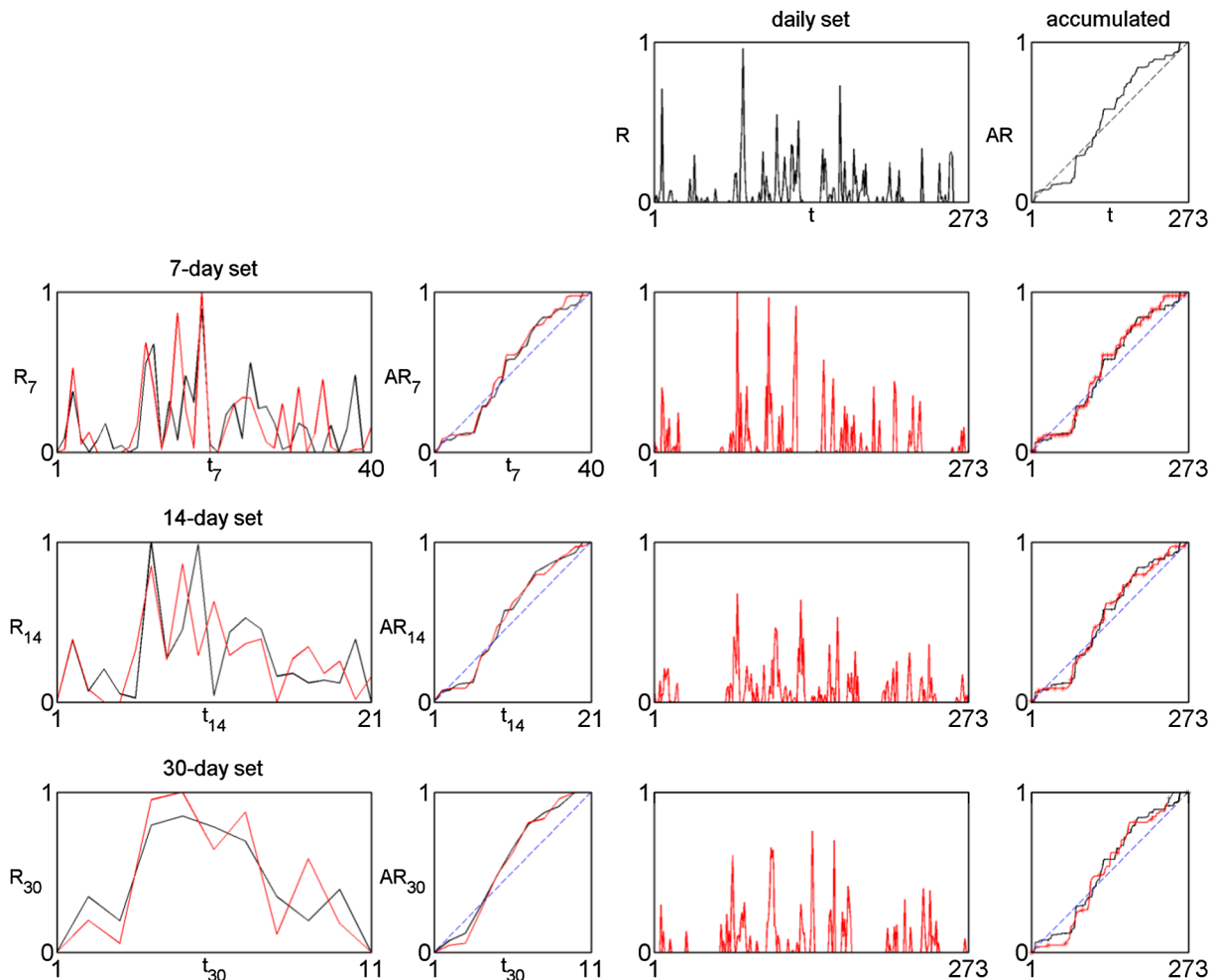


Fig. 3. Sets and accumulated records associated with rainfall gathered at Laikakota, Bolivia, during water year 1966. Observations (top row right); FM fits at coarse resolutions (three bottom rows left); and corresponding downscalings at the daily scale (three bottom rows right). The aggregation scales for the coarse records are 7, 14 and 30 days. Measurements are shown in black and FM-related information in gray.

Table 1
Error statistics for rainfall and streamflow FM downscales. Refer to the list of acronyms as defined in the text.

Set	Scale	$REAC$	$MEAC$	$NSED_C$	$REAF$	$MEAF$	$NSED_F$	$NSEA$	$NSEH$	$NSEE$	$PD90$	NZ
Rainfall Laikakota 1966	7	3.1	8.7	0	3.1	8.7	-1	-32	100	45	90	202(174)
	14	2.8	6.0	11	3.0	9.2	-70	28	99	56	93	163(174)
	30	3.1	6.3	60	4.3	11.3	-103	-19	99	90	92	201(174)
Rainfall Tinkham 1995	7	2.9	8.2	-16	2.9	9.3	-27	-29	98	56	95	199(18)
	14	3.0	9.6	19	3.1	9.6	-60	53	99	97	91	192(198)
	30	2.0	4.8	79	3.1	9.3	-111	-15	100	81	90	226(198)
Streamflow Sacramento 2005	7	0.7	1.5	84	0.7	1.5	73	96	90	100	90	
	14	0.6	3.9	94	0.9	3.9	41	90	97	100	88	
	30	0.7	3.2	98	1.2	3.2	60	84	90	100	90	
Streamflow Sacramento 2008	7	0.8	2.2	82	0.8	2.2	73	94	89	95	89	
	14	0.6	2.5	95	0.8	2.5	58	92	78	91	86	
	30	0.6	2.5	98	1.0	2.5	72	95	73	98	87	

6.3%, with the more complex set at the 7-day scale providing the largest deviation due to noticeable disparities by the end of the records, as seen in the second column and second row in Fig. 3. The closer renderings on biweekly and monthly scales are corroborated by the positive Nash-Sutcliffe efficiencies for the data in Table 1 ($NSED_C$), which are non-trivial to achieve for such highly-intermittent records (Maskey et al., 2016a). However, the value of zero for such an attribute at the 7-day aggregation scale confirms the complexity of rain at the weekly scale.

The third column and from the second to the fourth rows of Fig. 3 show the specific FM downscaling patterns obtained at the daily scale. As may be seen, the downscaled sets have intermittent textures similar to that of the original records and a reasonable following of the accumulated records. This is especially the case for the FM disaggregations

found from data gathered every 7 and 14 days. As may be corroborated from the statistical information in Table 1 (sixth to eighth columns), although the root mean square errors at the daily (finer) scale ($REAF$) remain close to the values found from the optimization exercises at the coarser resolutions (from 3 to 4.3%), the performance steadily degrades when the starting records to be fitted are coarser. Specifically, the maximum errors in accumulated sets at the daily scale ($MEAF$) increase from 8.7 up to 11.3% at the 30-day scale; and the Nash-Sutcliffe efficiencies for the daily rainfall data ($NSED_F$) decay and become increasingly negative, indicating the intrinsic difficulty in approximating rainfall sets.

Notice that, while these trends are to be expected (for a coarser scale implies usage of less information), a comparison with an FM encoding of the actual set at the daily scale is required to truly gauge the

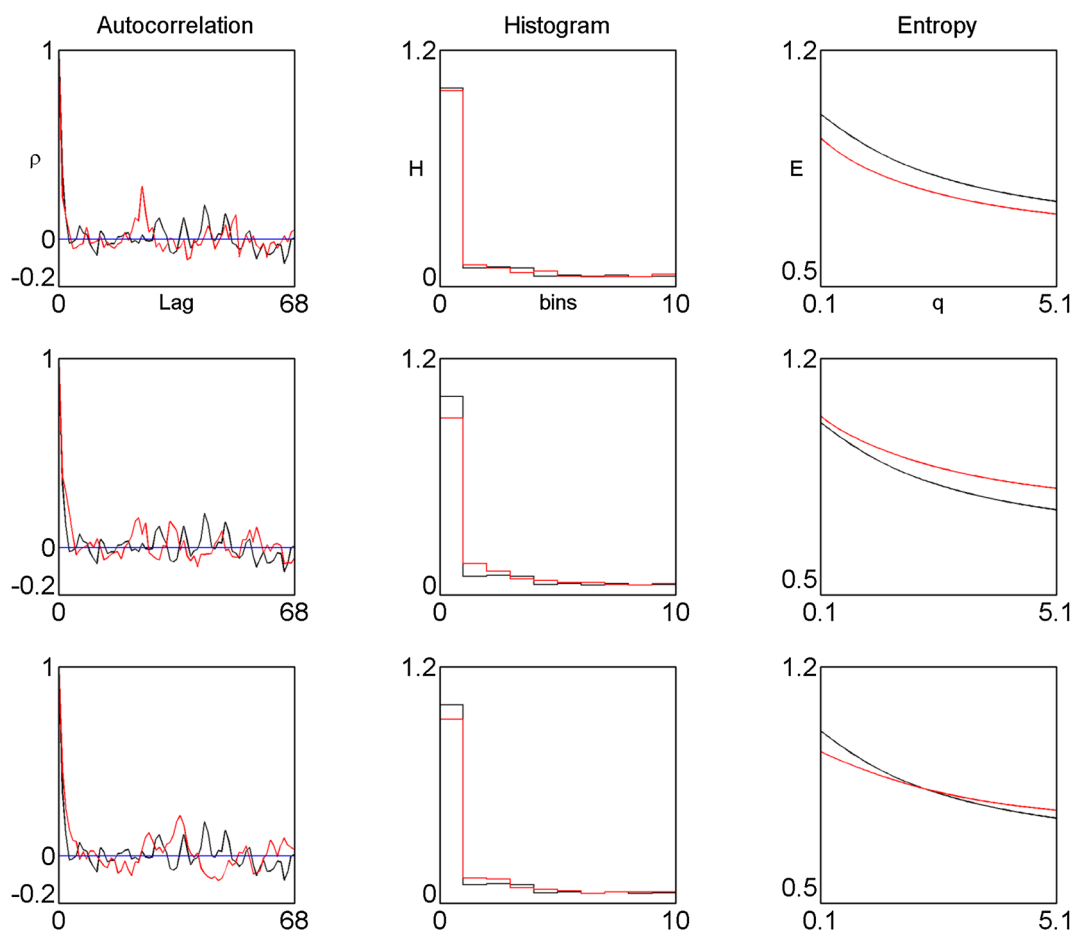


Fig. 4. Autocorrelation, histogram and entropy comparison for FM downscales in Fig. 3. Measurements are shown in black and FM-related information in gray.

goodness of an FM disaggregation. As the latter (i.e., optimizing at the daily scale) may be achieved with REA_F and MEA_F values of 1.4 and 4.4%, respectively (Maskey et al., 2016a), the obtained downscaled patterns having statistics that are at least twice such numbers (see Table 1) are not as tight to the records as possible. Notice, however, that the obtained patterns (even from accumulated data every 30 days) do look reasonable (see Fig. 3), which implies that they may be considered at least as suitable simulations of the highly variable rainfall data at the site.

Fig. 4 shows the statistical information regarding the obtained daily downscales at Laikakota as compared with the daily records. Such are (left to right), the autocorrelation function (i.e., lag vs. ρ), the histogram (i.e., bins vs. H , with a total of 10 bins based on the scale of the records and placing an FM value larger than the maximum in the last bin if needed), and the Rényi entropy function (i.e., q vs. E) for the three FM daily sets presented in Fig. 3 in the same order, 7-, 14-, and 30-day scales from top to bottom. As may be seen, this information corroborates that all FM-based downscales (in gray) are comparable as: (a) their autocorrelation functions follow the overall decay present in the records (black); (b) their histograms are rather close to the one of the records (with the one from 7-days being a bit better); and (c) their entropies exhibit similar decays, even if they are noticeably imperfect (with the one based on 30-days being less biased). These trends are reflected in the Nash-Sutcliffe efficiencies for these attributes (see Table 1): (a) negative values for autocorrelations ($NSEA$) that reflect the high variability and near zero values for correlations; (b) values

close to one hundred percent for histograms ($NSEH$); and (c) medium numbers for entropies ($NSEE$), with the FM representation based on 30-day aggregations being better as seen graphically.

Finally, it is worth comparing the three downscaled sets at the Laikakota site based on some extreme information, for both large and small values. In this regard, the last two columns in Table 1 include, first for large values, the percent histogram mass in FM sets corresponding to the 90% decile of the records ($PD90$) and, second for small values, the number of zeros in a set (NZ) comparing observed records with FM downscales, with the former shown in parentheses. As seen, and as hinted from the histograms, the FM-downscaled set from records every 7 days is a bit better in $PD90$, as instead of fitting the prescribed 90%, the other two FM representations have higher but close values of 93 and 92%. Regarding the number of zeros, the set found via 14 days is found to be better (163 vs. 174), with the other disaggregation scales yielding sets having more zeros than those found in the records (201 and 202 vs. 174).

4.2. Rainfall set from Tinkham, Washington

Figs. 5 and 6 show the counterparts of Figs. 3 and 4 for rainfall records gathered in Tinkham, Washington State, for water year 1995. As seen, at the daily scale (first row of Fig. 5), this series, made of 365 values, when compared with the one for Laikakota in Fig. 3, appears to be “more complex.” This highly-intermittent set contains many up and down swings and has a large peak within the first two months, which is

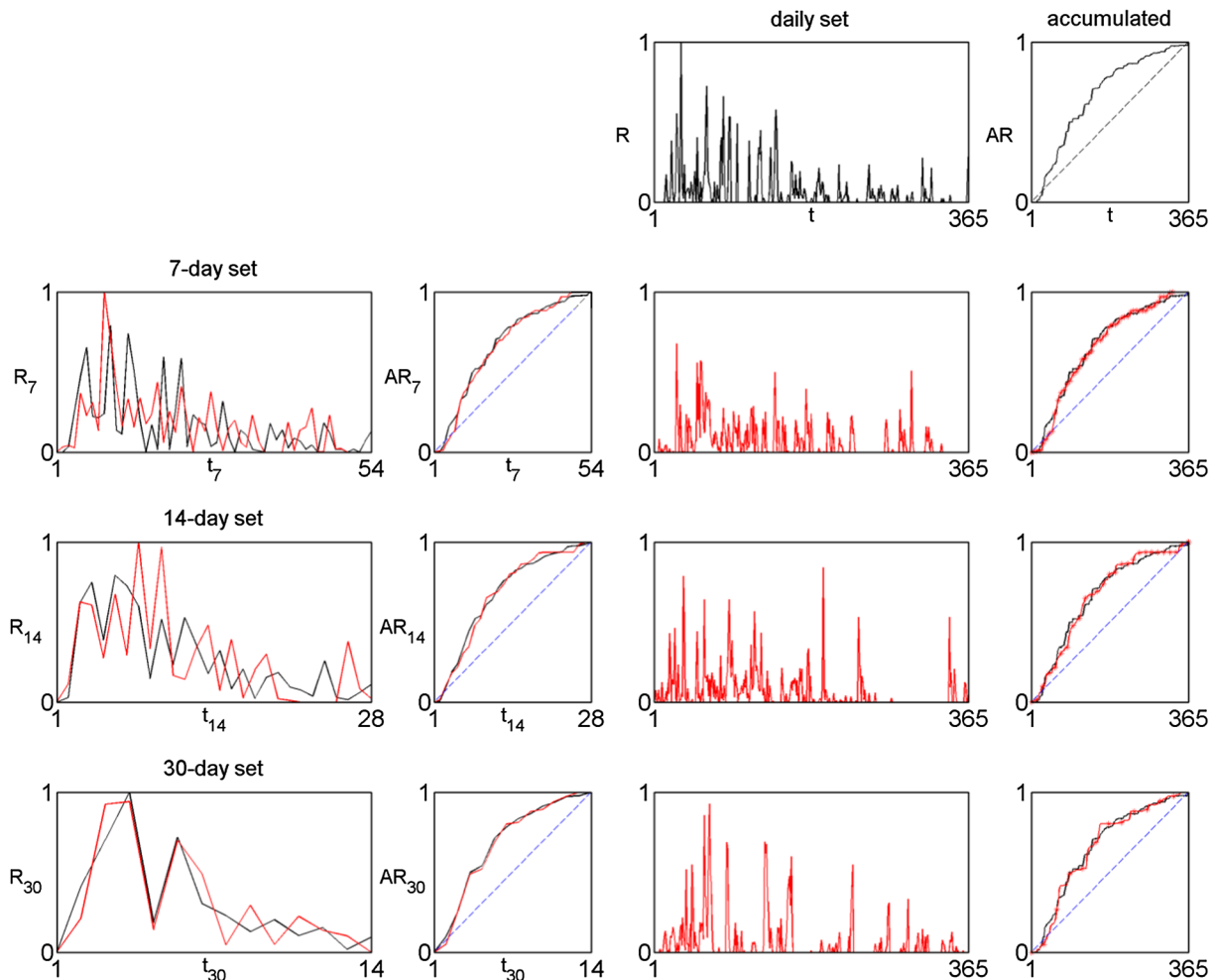


Fig. 5. Sets and accumulated records associated with rainfall gathered at Tinkham, Washington, during water year 1995. Observations (top row right); FM fits at coarse resolutions (three bottom rows left); and corresponding downscalings at the daily scale (three bottom rows right). The aggregation scales for the coarse records are 7, 14 and 30 days. Measurements are shown in black and FM-related information in gray.

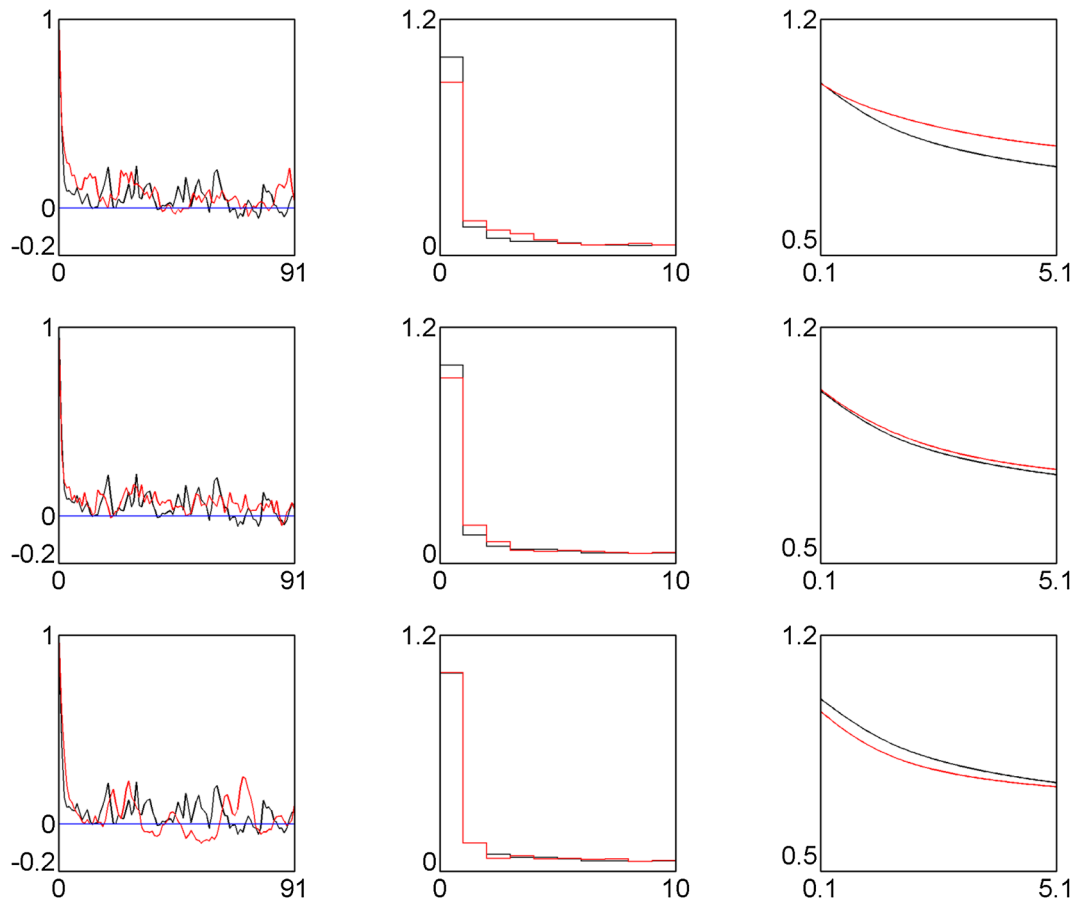


Fig. 6. Autocorrelation, histogram and entropy comparison for FM downscales in Fig. 5. Measurements are shown in black and FM-related information in gray.

followed by a collection of several peaks exhibiting mainly a decreasing trend until the middle of the water year. As may be seen on the left of Fig. 5, when the records are aggregated over 7, 14, and 30 days, the decaying trend from the main peak to the future remains, but, as expected, the increased smoothing makes the patterns less variable.

Similar to the case for Laikakota, usage of a threshold on a derived measure, obtained via a fractal function generated by the iteration of three maps (as in Fig. 1 but with parameters different from such a figure), results in reasonable FM representations at the 7-, 14-, and 30-day resolutions (first and second columns of the bottom three rows in Fig. 5), with FM parameters included in the fourth to sixth rows of Appendix A. Even though the locations of the FM peaks (in gray) are not identical to those of the records (in black) and the actual magnitudes are overestimated (especially at the 14-day resolution), all sets do exhibit similar textures and result in very close fittings of the accumulated records. Such reasonable fittings on coarser scales are supported by the smaller values of REA_C and MEA_C (see Table 1 for Tinkham), with 2.9 and 8.2% at the weekly scale, 3.0 and 9.6% at the biweekly scale, and 2.0 and 4.8% at the monthly scale. Notice how these numbers are comparable to those found for the Laikakota site, even if the records for Tinkham reflect a longer water year length equal to the whole calendar year. The closer renderings on biweekly and monthly scales give rise, as previously found for Laikakota, to positive Nash-Sutcliffe efficiencies at those scales (see $NSED_C$), but the negative value obtained at the 7-day scale confirms the complex nature of the records.

Although noticeable differences in daily downscales at all resolutions are observed in the third column of Fig. 5, the last column there reveals that all disaggregated FM representations, using exactly the same parameters optimized at the coarser scales, yield equally good accumulated sets. Certainly, to the naked eye, the three FM mass functions follow the accumulated trends well, and such is reflected by

the rather small and similar values of REA_F and MEA_F (see center of Table 1), which are close to those obtained by the optimization exercise, with values of about 3.0 and 9.6%, respectively. These numbers, when compared with encodings of the daily records themselves, reveal that the downscaled sets do not follow the accumulated records as closely as it may be modeled by an FM fit at the daily scale. This is the case as the smallest REA_F and MEA_F values possible via the FM approach are 1.1 and 4.4% (Maskey et al., 2016a), which, once again, are less than half of what the downscaled sets portrayed in Fig. 5 yield. This result is consistent with what was reported earlier for the rainfall set from Laikakota.

Although the accumulated sets look similar, surely the naked eye cannot be fooled while comparing the FM sets themselves on the third column in Fig. 5. As mentioned earlier, these sets are clearly different and no doubt exhibit distinct intermittencies. In this regard, what was found at Laikakota extends to Tinkham regarding the Nash-Sutcliffe efficiency of the records at the finer resolution. Such a statistic, $NSED_F$, reflects the complexity of the records and the FM sets and degrades with an increased scale of the records, from -27 at the weekly scale to -111 at the monthly scale (See Table 1), which as mentioned earlier is not uncommon even while encoding the information (Maskey et al., 2016a).

As illustrated in Fig. 6 for the Tinkham rainfall set, the quickly decaying autocorrelation function, the concentration of the histogram on small values, and the decrease of the Rényi entropy function are nicely preserved for this rainfall set by all FM representations. These features, not included in the optimization exercise, give rise to low Nash-Sutcliffe efficiencies for autocorrelations ($NSEA$) (once again due to rather small statistically insignificant oscillatory values) and to high Nash-Sutcliffe efficiencies for both the histogram and the entropy function ($NSEH$ and $NSEE$), with values that are higher than 98% and

56%, respectively, and with the set based on the biweekly scale yielding a remarkable preservation of the entropy (see Table 1). As may be seen on the last columns of Table 1 for the extreme information related to the Tinkham sets, the large values at a 90% level (PD_{90}) are over-estimated by the FM downscales at the weekly and biweekly scales (95 and 91%, respectively), although such is perfectly fitted at the monthly scale. As found for Laikakota, there is no clear relation between the fitting of large and small values, for the number of zeros recorded in the set, 198 days, may be under- or over-estimated by the FM representations, i.e., 199, 192 and 226 days (see Table 1). Altogether, however, the obtained downscales may be termed adequate to represent rainfall at this site at the daily scale.

4.3. Remarks on rainfall downscaling

The above analysis and results of downscaling of rainfall data from three coarser scales (weekly, biweekly, and monthly) to daily scale for the two distinct sites in different countries (Laikakota, Bolivia and Tinkham, Washington State, USA) reveal that the FM approach is capable of representing the overall trends and intermittent features of the rather complex rainfall records in a reasonable, albeit imperfect, way. Although the Nash-Sutcliffe values obtained for the downscaled data at the daily scale may be negative, compared to the positive values of greater than 63.8% for the weekly-aggregated records found from daily encodings (Maskey et al., 2016a), the geometric shapes of the downscaled data do provide relevant and certainly useful information, at the very least from a simulation point of view.

Clearly, the usage of other “solutions” of the optimization exercise provides yet other alternative FM representations, for various scales, that may also be used in practical applications for planning and design purposes. Fig. 7 illustrates such an idea based on the weekly scale at the Tinkham site for three other “solutions” of the associated inverse problem, as included in the seventh to ninth rows in Appendix A, and from top to bottom as in the figure. The modeled daily sets in Fig. 7 have similar textures to those shown in Fig. 5, and their statistical features (not presented here) are also found to be in reasonable agreement with those presented in Table 1 for the other sets. All these results suggest that the FM approach yields sensible realizations akin to random ones obtained via stochastic disaggregation methods, even if the magnitude of the peaks shown is smaller. These, therefore, are clearly alternative representations that, while following the overall location of the rain throughout the year, still maintain the highly intermittent nature of the records.

5. Downscaling of streamflow sets

This section reports the analysis of streamflow downscaling using the FM approach. For this purpose, streamflow data from the Sacramento River, measured near Freeport, California (USGS station 11447650) is considered. Similar to what was done for rainfall in the previous section, the FM approach is applied to downscale streamflow to the daily scale from 7-, 14-, and 30-day aggregated sets. Two different water years having distinct geometries are considered to validate the method: years 2005 and 2008, both from October 1 to September 30 of the following year. For the daily data set (and, consequently, the aggregated 7-, 14-, and 30-days), a constant base flow equal to the minimum in the records is subtracted from the raw daily data, so that the FM approach may better fit those records.

After normalizing an obtained streamflow sets, downscaling of streamflow is attempted using a fractal interpolating function based on the iteration of three maps, adding a local smoothing, just for appearance purposes and based on our previous experience (Maskey et al., 2016b), of 5 days, as illustrated in Fig. 2. At the end, the FM representations depend on only 9 free parameters, as the smoothing is always set at the 5-day level. The representations, whose parameters are included in the last six rows of Appendix A, hence correspond to a

compression ratio (at the daily scale) of 365/9 or 40:1.

To further illustrate the abilities of the FM approach to disaggregate streamflow (and perhaps other mildly intermittent hydrologic) records, the results that follow include a modification to the definition of optimality at the coarse scale. While calculations are guided by the same objective function as in the rainfall studies earlier (i.e., the root mean square error of accumulated coarse data $REAC$ and subject to due penalties), the “best” results are defined herein from the minimum of the maximum error in accumulated coarse data $MEAC$. This is done in the spirit of the Kolmogorov-Smirnov test for comparing two distributions and as a means of performing a sensitivity analysis on the choice of the objective function.

Figs. 8 and 9 present the streamflow downscaling results for water year 2005 and Figs. 10 and 11 include the results for water year 2008. Figs. 8–11 are similar to Figs. 3–6 presented earlier for rainfall, with the distinction that the observed records at the fine scale are now plotted on top of the obtained downscales. For the two water years, while Figs. 8 and 10 present the original (daily) data sets and their accumulated sets (with actual records in black and FM representations in gray), Figs. 9 and 11 display their respective autocorrelation, histogram and entropy. In what follows, a step by step description of the obtained FM downscaled sets for the two water years is presented.

5.1. Streamflow set from the Sacramento River: water year 2005

Fig. 8 shows the original data (in black) at the daily scale (right) and the aggregated weekly, biweekly and monthly data of streamflow records (minus base flow) for the water year 2005. As seen, these records are much less intermittent when compared to the rainfall sets studied

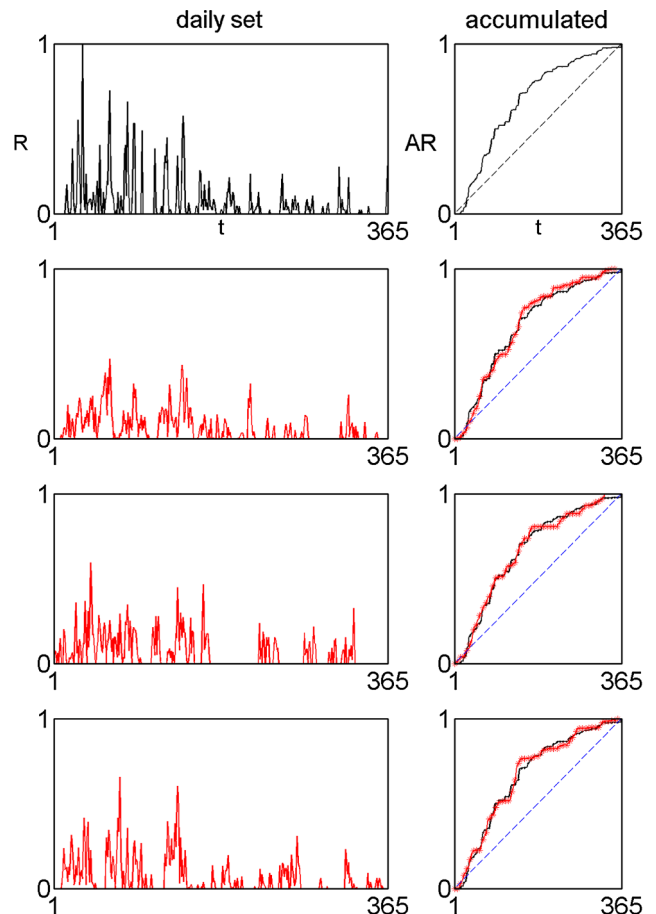


Fig. 7. Alternative daily downscaled sets (in gray) based on FM fits at the 7-day scale for the water year 1995 at the site at Tinkham.

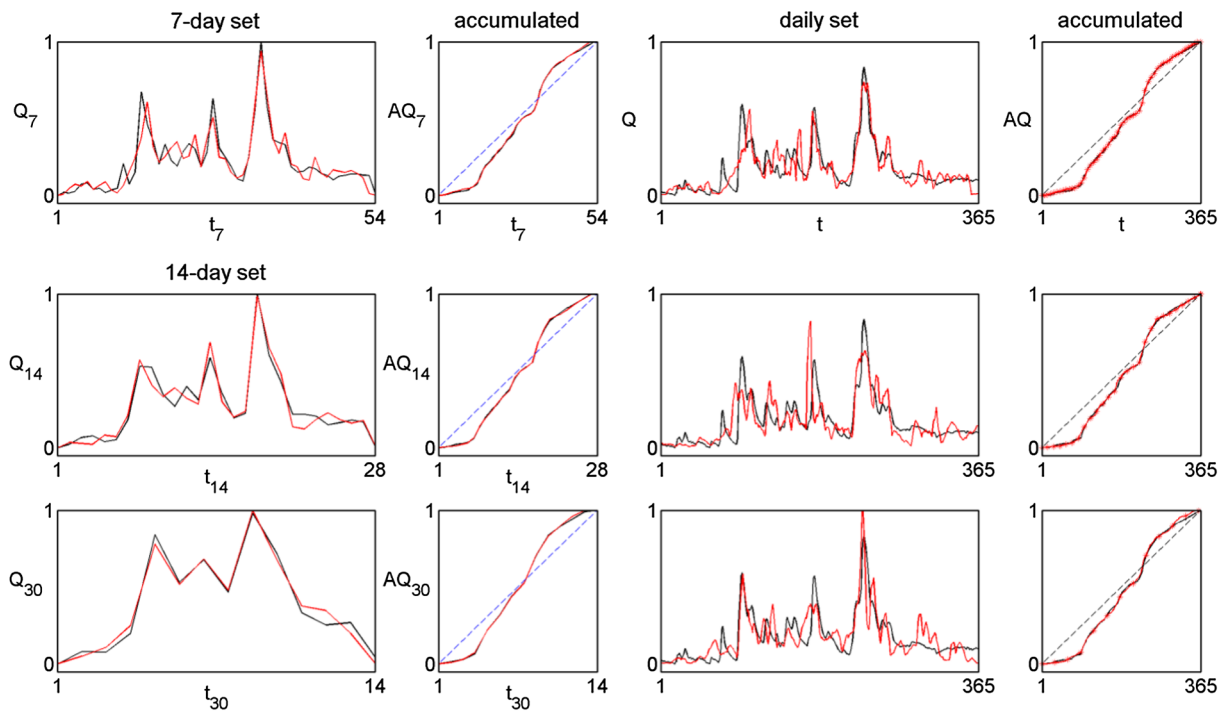


Fig. 8. Sets and accumulated records associated with streamflow gathered at Sacramento River, during water year 2005. FM fits at coarse resolutions (three rows left) and corresponding observations and downscalings at the daily scale (three rows right). The aggregation scales for the coarse records are 7, 14 and 30 days. Measurements are shown in black and FM-related information in gray.

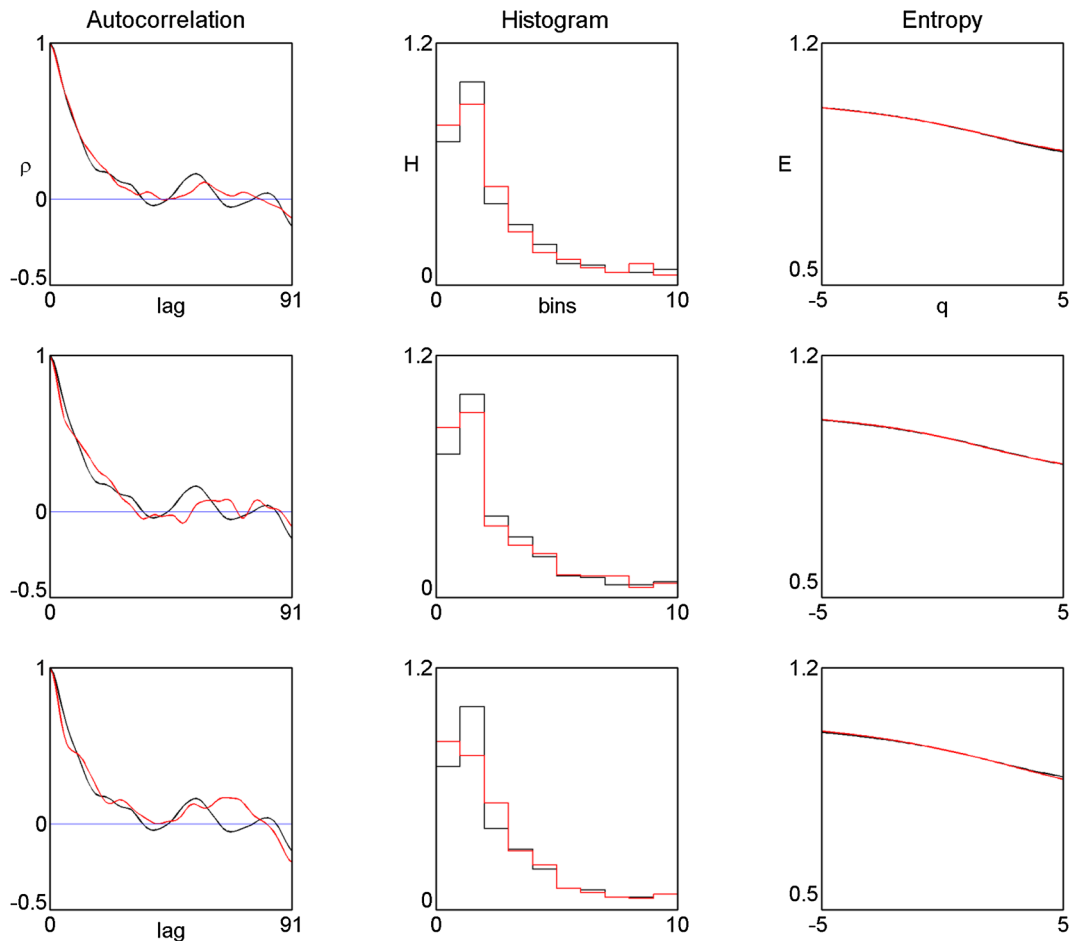


Fig. 9. Autocorrelation, histogram and entropy comparison for FM downscales in Fig. 8. Measurements are shown in black and FM-related information in gray.

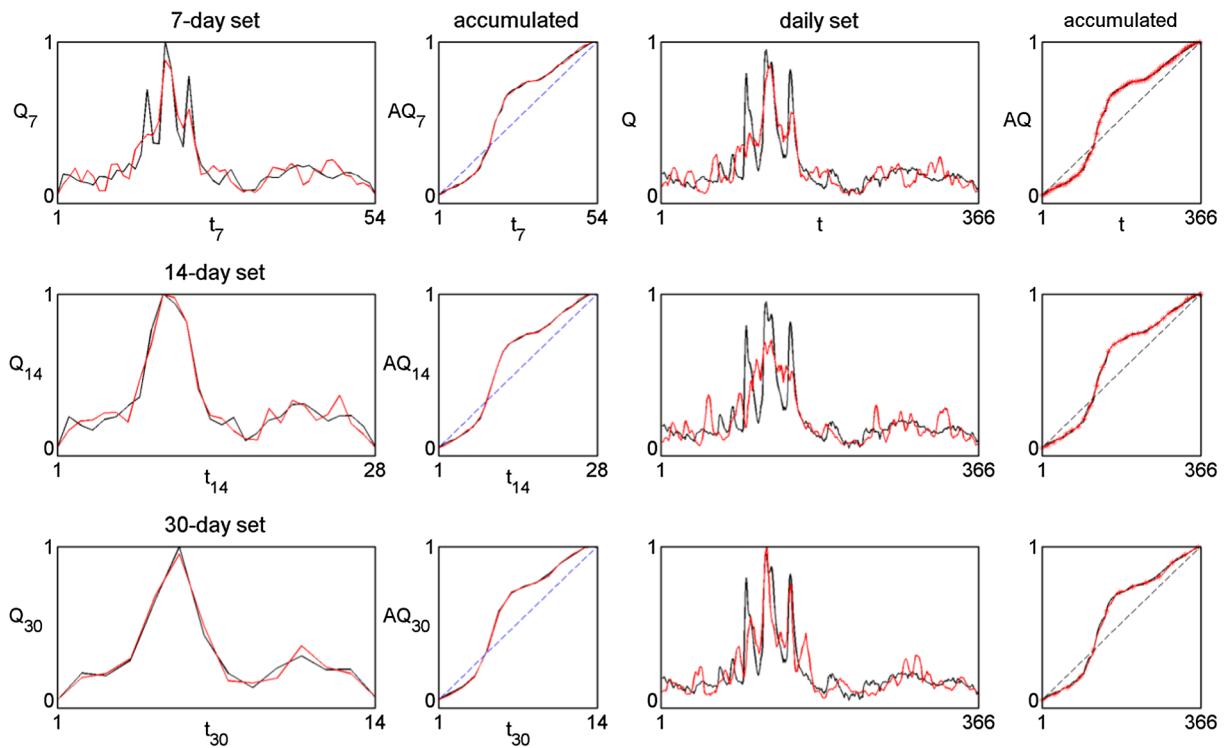


Fig. 10. Sets and accumulated records associated with streamflow gathered at Sacramento River, during water year 2008. FM fits at coarse resolutions (three rows left) and corresponding observations and downscalings at the daily scale (three rows right). The aggregation scales for the coarse records are 7, 14 and 30 days. Measurements are shown in black and FM-related information in gray.

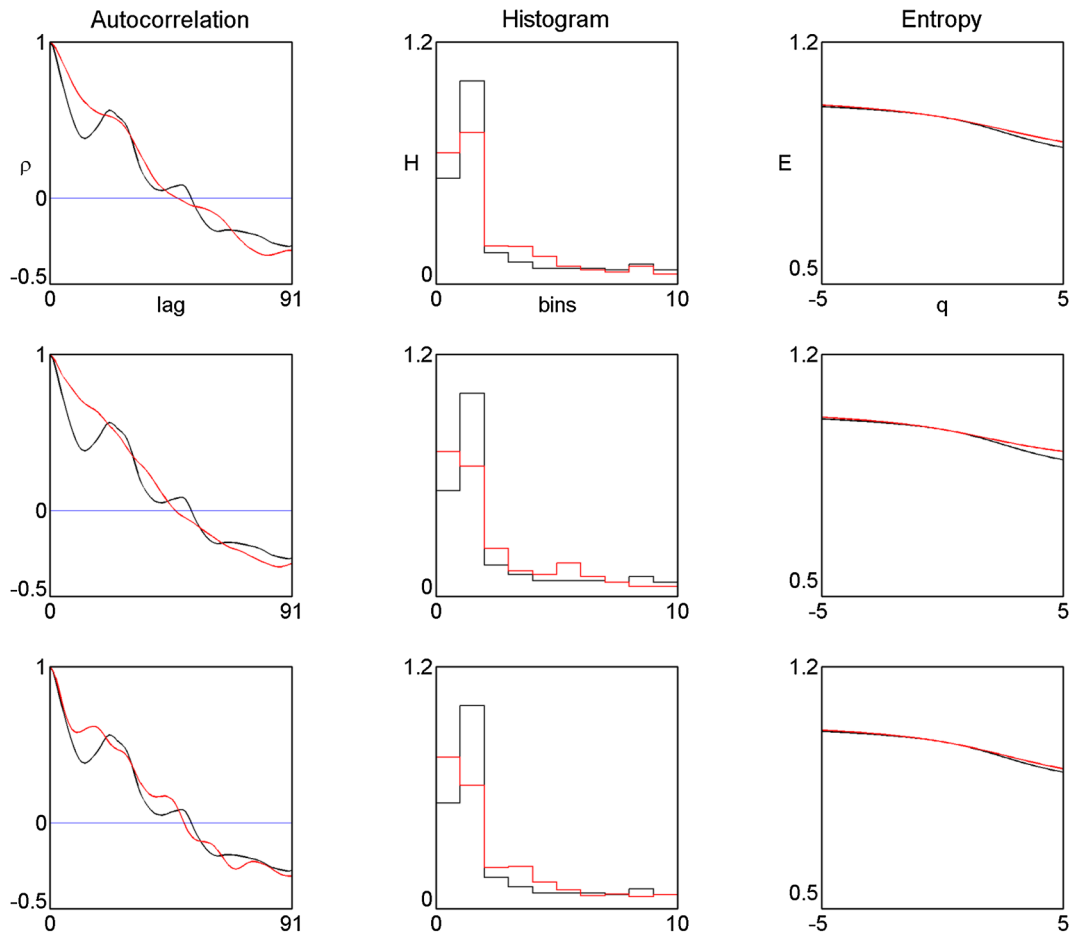


Fig. 11. Autocorrelation, histogram and entropy comparison for FM downscalings in Fig. 10. Measurements are shown in black and FM-related information in gray.

earlier, and contain (at the resolutions shown) three main peaks located around the central portion of the water year, with the last one being the largest. Fig. 8 also includes the three “optimal” FM representations (in gray) found from the three coarse scales (left blocks), and the corresponding FM disaggregations (in gray) at the daily scale (right blocks). Notice the rather faithful FM fits for all coarse scales (on the left), which result in accurate preservations of the main peaks in the sets. This is corroborated by the error measures included in Table 1, third horizontal block.

As seen, the root mean square error in accumulated sets (REA_C) and maximum error in accumulated sets (MEA_C) (the new optimal) are always less than a mere 0.7 and 3.9% for all coarse representations, and the Nash-Sutcliffe efficiencies for those coarse records at all scales ($NSED_C$) are always above a healthy 84%. Of all coarse representations (and somewhat surprisingly given the opposite trends found in rainfall), the one found for weekly records is the best, with REA_C equal to 0.7% and MEA_C equal to just 1.5%. This is certainly much better than what was found for rainfall data (i.e., four times in the former and about 6 times in the latter attribute). Altogether, the Nash-Sutcliffe efficiencies $NSED_C$ do increase with coarser records, as reported in the rainfall cases before.

Fig. 8 also shows (right blocks) the downscaled patterns at the daily scale. As seen, the obtained set based on the weekly scale (top) gives the best following of the major peaks, as the first one is missed just by a few days and the two others are preserved almost perfectly in timing and magnitude. The daily representations emanating from 14 and 30 days do exhibit patterns that follow the main peaks, but with noticeable over-estimation. For instance, the one from the biweekly scale over-predicts the second peak, while the one from the monthly scale over-predicts the third peak. Altogether, the accumulated daily sets (from the downscaled sets) rather closely follow those at the fine scale, i.e., the original daily records. This is confirmed in Table 1 (third block, center columns), for the statistics at the fine scale (REA_F and MEA_F), which are less than 1.2 and 3.9%, respectively, and comparable to what is found while encoding the daily records themselves. Notice that errors at the coarse and fine scales corresponding to the 7-day scale are identical, i.e., $REA_C = REA_F = 0.7\%$ and $MEA_C = MEA_F = 1.5\%$, indicating an excellent preservation of the accumulated records by such downscales. Observe also that while the maximum accumulated errors are maintained for the other two sets (i.e., $MEA_C = MEA_F$), the process of disaggregation degrades the root mean square errors on the accumulated streamflow (i.e., $REA_C < REA_F$). Obviously, the downscaled daily data from the 7-day scale most closely resembles the original daily flows and such is also reflected by the Nash-Sutcliffe efficiency for the daily disaggregated data ($NSED_F$), which remains high at a rather healthy 73%.

The statistical attributes in Fig. 9 further imply that the FM-based disaggregation approach performs very well at all aggregation scales considered. Notice the close following of the record’s autocorrelation function and histogram (albeit not perfect) and the rather close fits (and almost perfect) of the entropy function. This is also reflected in Table 1 (third block, right columns), by the rather high Nash-Sutcliffe efficiency indices for such attributes that are quite close to 100% and the excellent fit of the extreme records at the 90% level. It is worth mentioning that it is hard to distinguish the quality of the three downscales just based on these statistics, an indication that the geometric FM method provides good downscales for this water year.

5.2. Streamflow set from the Sacramento River: water year 2008

Fig. 10 presents the key graphs of the results of FM-fits and downscales for water year 2008. As seen, the original daily records (in black) contain three sharp peaks in succession, which remain at the 7-day scale but that are smoothed out at the 14- and 30-day scales. As observed on the left blocks in Fig. 10, the FM representations of the coarse records are excellent, both in accumulated records and in the data, with the latter particularly good for the two smoothed sets (i.e., 14-day and

30-day). This is reflected in Table 1 (last block, left columns) by comparable and small values of REA_C and MEA_C (i.e., less than 0.8 and 2.5%, respectively) and by $NSED_C$ values that range, as the aggregation increases, from 82 to 95 to 98%, certainly remarkable numbers.

Regarding the downscaled daily comparisons (right block of Fig. 10), while the accumulated sets yield, by eye, very similar behavior (corroborated by close values of REA_F and MEA_F , which are close to those at the coarse resolution and to those found from FM encodings of the daily set; see central columns of the last block on Table 1), the sets themselves have varying qualities, as follows. The disaggregated pattern found for 7 days, emanating from an FM fit that captures well the last two sharp peaks, not surprisingly preserves the timing and overall shape of the same peaks. The pattern associated with the 14-day scale yields essentially similar shapes at the fine (right) and coarse (left) resolutions, and, as a consequence, it misses the structure of the three peaks, even if the overall volume is correct. Finally, the downscaled daily set based on the 30-day FM disaggregation surprisingly captures the overall sense of the three peaks on the daily records. Curiously, the “optimal” solution spanning from the 30-day scale is equally good as the one done on a weekly basis, as is seen in Table 1 for the NSD_F attribute, which exceeds a rather high magnitude of 72% in both cases.

The graphs in Fig. 11 show the statistical information of the FM downscaled data, and the pertinent statistical qualifiers are presented in Table 1 (last horizontal block, right columns). As seen, all the auto-correlations generally follow the overall decay in the records, although they miss the first noticeable dip. The $NSEA$ values are rather good, with greater than 92%, and better than what was reported earlier for the 2005 streamflow set. The histograms for the downscaled data for water year 2008 show, in general, more variation than those for water year 2005, and degrade in quality as the scale is increased (contrary to what was found for water year 2005). The $NSEH$ values decay from 89 to 78 and to 73, and, as such, the set implied by the 30-day scale no longer competes with the one based on 7 days, although the $PD90$ values are close to one another (89 vs. 87). As seen in Fig. 11 and Table 1, all sets provide close fittings of the entropy function of the records, with $NSEE$ values in excess of a high 91%.

In summary, the application of the FM-based disaggregation model to streamflow records yield very good results, and much better than what was found for rainfall. These very good results for streamflow are to be expected given the smoother nature of the records when compared to rainfall.

6. Concluding remarks

This study has proposed a deterministic geometric fractal-multi-fractal (FM) approach to downscale hydrologic records, specifically rainfall and streamflow. The proposed approach for temporal downscaling is an adaptation of the original FM approach for encoding of records (Puentes, 1996), which adds a threshold for rainfall and local smoothing for streamflow. By studying two rainfall records (from Llakota, Bolivia and Tinkham, Washington State, USA) and two streamflow records (from the Sacramento River, USA), the FM-based method has been shown to be an effective and efficient tool for downscaling, especially for streamflow sets. As the notions are based on accumulated records, it is envisioned that the geometric downscaling approach may also be applied using data gathered at a coarse scale over not just one but multiple years.

The results from this study clearly indicate that the deterministic FM geometric procedure, when coupled with an effective optimization procedure for the inverse problem for a given target set at a coarse resolution, not only encodes coarse-scale records (i.e., weekly, bi-weekly, and monthly) but also generates plausible downscale representations, at least for simulation purposes, at the finer scale (i.e., daily). Such a novel approach, yielding compression ratios as high as 37:1 for rainfall sets and 40:1 for streamflow records, may, therefore, supplement existing stochastic downscaling methods, supporting the

notion of hidden determinism in natural complexity (Puente, 1996; Puente and Sivakumar, 2007).

The proposed downscaling technique, in conjunction with simulations that may be obtained via the FM approach (Maskey et al., 2016c, 2017), may certainly increase the flexibility for generating time series in a multisite or multi-season framework as done by other approaches (e.g., Salas et al., 1995). As the same number of FM parameters define both coarse and fine sets, the evolution of the inherent complexity in the physical processes may be studied based on them. It is envisioned that a sensible application of the FM-based disaggregation could be the temporal downscaling of coarse-scale outputs from global circulation models (GCMs) to catchment-scale hydrologic variables, in order to assess the impacts of climate change on hydrology and water resources in a region.

Appendix A

Parameters for FM downscaling of rainfall and streamflow.

Figure (scale)	FM parameters									
	x_1	x_2	y_1	y_2	d_1	d_2	d_3	p_1	p_2	ϕ_v
3(7)	0.281	0.784	1.122	-2.628	-0.631	0.141	0.265	0.522	0.020	0.192
3(14)	0.193	0.855	1.422	-2.155	-0.500	-0.629	0.301	0.452	0.080	0.155
3(30)	0.120	0.753	2.238	-5.000	-0.517	-0.398	0.367	0.405	0.040	0.185
5(7)	0.000	0.321	-4.260	-5.000	0.202	0.245	0.455	0.285	0.103	0.096
5(14)	0.353	0.833	-2.131	-1.725	0.740	0.164	-0.064	0.634	0.121	0.074
5(30)	0.249	0.508	4.004	-1.843	0.213	0.498	-0.154	0.046	0.593	0.053
7(7)	0.174	0.782	4.685	-2.145	0.252	-0.263	0.821	0.202	0.308	0.250
7(7)	0.022	0.317	4.720	-3.550	-0.194	-0.845	0.594	0.305	0.093	0.158
7(7)	0.055	0.719	2.685	0.651	0.662	0.493	-0.118	0.474	0.358	0.200
8(7)	0.297	0.519	3.348	1.296	0.277	-0.237	-0.789	0.509	0.167	-
8(14)	0.375	0.560	2.988	4.999	0.303	-0.970	0.169	0.150	0.265	-
8(30)	0.384	0.771	-4.060	-4.904	-0.195	-0.913	-0.429	0.390	0.246	-
10(7)	0.398	0.780	2.413	-2.414	-0.567	-0.389	0.408	0.373	0.318	-
10(14)	0.389	0.817	3.725	-3.525	-0.531	-0.376	0.469	0.358	0.380	-
10(30)	0.273	0.912	-4.723	-2.403	0.516	-0.310	-0.874	0.245	0.438	-

References

Alvisi, S., Ansaloni, N., Franchini, M., 2015. Comparison of parametric and nonparametric disaggregation models for the top-down generation of water demand time series. *Civ. Eng. Environ. Syst.* 1–19. <https://doi.org/10.1080/10286608.2015.1126823>.

Barnsley, M.F., 1988. *Fractals Everywhere*. Academic Press, San Diego.

Bras, R.L., Rodríguez-Iturbe, I., 1976. Rainfall generation: a nonstationary time-varying multidimensional model. *Water Resour. Res.* 12 (3), 450–456.

Connolly, R.D., Schirmer, J., Dunn, P.K., 1998. A daily rainfall disaggregation model. *Agri. For. Meteorol.* 92, 105–117.

Cortis, A., Puente, C.E., Sivakumar, B., 2009. Nonlinear extensions of a fractal-multifractal approach for environmental modeling. *Stoch. Environ. Res. Risk Assess.* 23 (7), 897–906.

Cortis, A., Puente, C.E., Huang, H.H., Maskey, M.L., Sivakumar, B., Obregón, N., 2013. A physical interpretation of the deterministic fractal-multifractal method as a realization of a generalized multiplicative cascade. *Stoch. Environ. Res. Risk Assess.* 28 (6), 1421–1429.

Fernández Martínez, J.L., García Gonzalo, E., Fernández Álvarez, J.P., Kuzma, H.A., Menéndez Pérez, C.O., 2010. PSO: a powerful algorithm to solve geophysical inverse problems Application to a 1D-DC resistivity case. *J. Appl. Geophys.* 71 (1), 13–25.

Fowler, H.J., Blenkinsop, S., Tebaldi, C., 2007. Linking climate change modelling to impacts studies: recent advances in downscaling techniques for hydrological modelling. *Int. J. Climatol.* 27 (12), 1547–1578.

Grace, R.A., Eagleson, P.S., 1966. The synthesis of short-time increment rainfall sequences. Report., Mass. Inst. of Technol. Hydrodyn. Lab., no. 91.

Güntner, A., Olsson, J., Calver, A., Gannon, B., 2001. Cascade-based disaggregation of continuous rainfall time series: the influence of climate. *Hydrol. Earth Syst. Sci.* 5, 145–164.

Gupta, V.K., Waymire, E., 1990. Multiscaling properties of spatial rainfall and river flow distributions. *J. Geophys. Res.* 95 (D3), 1999–2009.

Hershenson, J., Woolhiser, D.A., 1987. Disaggregation of daily rainfall. *J. Hydrol.* 95, 299–322.

Hoshi, K., Burges, S.J., 1979. Disaggregation of streamflow volumes. *J. Hydrol. Div.-ASCE*

Acknowledgements

The research leading to this article was supported by a JASTRO Award provided to the first author by the University of California, Davis. We are thankful to Ministerio de Medio Ambiente y Agua, Bolivia for providing rainfall records gathered at Laikakota and also to the team of National Resource Conservation Service for the availability of rainfall records in its web portal. Bellie Sivakumar acknowledges the financial support from the Australian Research Council (ARC) through the Future Fellowship grant awarded to him (FT110100328). The team of USGS service is also greatly appreciated for making the historical streamflow records available in its web portal. Comments from anonymous reviewers helped us improve the manuscript and are gratefully acknowledged.

105 (HY1), 27–41.

Huang, H.H., Puente, C.E., Cortis, A., Sivakumar, B., 2012. Closing the loop with fractal interpolating functions for geophysical encoding. *Fractals* 20 (3–4), 261–270.

Huang, H.H., Puente, C.E., Cortis, A., Fernández Martínez, J.L., 2013. An effective inversion strategy for fractal-multifractal encoding of a storm in Boston. *J. Hydrol.* 496, 205–216.

Koutsoyiannis, D., 1992. A nonlinear disaggregation method with a reduced parameter set for simulation of hydrologic series. *Water Resour. Res.* 28 (12), 3175–3191.

Koutsoyiannis, D., 1994. A stochastic disaggregation method for design storm and flood synthesis. *J. Hydrol.* 156 (1), 193–225.

Koutsoyiannis, D., 2003. Rainfall disaggregation methods: Theory and applications. In: *Statistical and Mathematical Methods for Hydrological Analysis*, Rome, pp. 1–23.

Koutsoyiannis, D., Xanthopoulos, T., 1990. A dynamic model for short-scale rainfall disaggregation. *Hydrol. Sci.* 35 (3), 303–322.

Koutsoyiannis, D., Onof, C., Wheeler, H.S., 2003. Multivariate rainfall disaggregation at a fine timescale. *Water Resour. Res.* 39, 1173. <https://doi.org/10.1029/2002WR001600>.

Kumar, D.N., Lall, U., Peterson, M.R., 2000. Multisite disaggregation of monthly to daily streamflow. *Water Resour. Res.* 36 (7), 1823–1833.

Lall, U., 1995. Recent advances in nonparametric function estimation: hydrologic applications. *Rev. Geophys.* 33 (S2), 1093–1102.

Lanza, L.G., Ramírez, J.A., Todini, E., 2001. Stochastic rainfall interpolation and downscaling. *Hydrol. Earth Syst. Sci.* 5 (2), 139–143.

Liu, J., Yuan, D., Zhang, L., Zou, X., Song, L., 2016. Comparison of three statistical downscaling methods and ensemble downscaling method based on bayesian model averaging in upper Hanjiang River Basin, China. *Adv. Meteorol.* doi:10.1155/2016/7463963.un.

Lorenz, E.N., 1963. Deterministic nonperiodic flow. *J. Atmos. Sci.* 20, 130–141.

Lovejoy, S., Schertzer, D., 2013. *The Weather and Climate: Emergent Laws and Multifractal Cascades*. Cambridge University Press, Cambridge.

Mandelbrot, B.B., 1982. *The Fractal Geometry of Nature*. Freeman, San Francisco.

Mandelbrot, B.B., 1989. Multifractal measures especially for the geophysicist. In: Scholz, C.H., Mandelbrot, B.B. (Eds.), *Fractals in Geophysics*. Birkhanser Verlag, Basel, pp. 1–42.

Maskey, M.L., Puente, C.E., Sivakumar, B., 2016a. Encoding daily rainfall records via

- adaptations of the fractal multifractal method. *Stoch. Environ. Res. Risk Assess.* 30, 1917–1931.
- Maskey, M.L., Puente, C.E., Sivakumar, B., 2016b. A comparison of fractal-multifractal techniques for encoding streamflow records. *J. Hydrol.* 542, 564–580.
- Maskey, M.L., Puente, C.E., Sivakumar, B., Cortis, A., 2016c. Deterministic simulation of highly intermittent hydrologic records. *Stoch. Environ. Res. Risk Assess.* <https://doi.org/10.1007/s00477-016-1343-2>.
- Maskey, M.L., Puente, C.E., Sivakumar, B., Cortis, A., 2017. Deterministic simulation of mildly intermittent hydrologic records. *J. Hydrol. Eng.* 22 (8), 04017026.
- Mejia, J.M., Rouselle, J., 1976. Disaggregation models in hydrology revisited. *Water Resour. Res.* 12 (2), 185–186.
- Meneveau, C., Sreenivasan, K.R., 1987. Simple multifractal cascade model for fully developed turbulence. *Phys. Rev. Lett.* 59, 1424–1427.
- Nash, J., Sutcliffe, J.V., 1970. River flow forecasting through conceptual models part I—a discussion of principles. *J. Hydrol.* 10 (3), 282–290.
- Obregón, N., Puente, C.E., Sivakumar, B., 2002a. Modeling high resolution rain rates via a deterministic fractal–multifractal approach. *Fractals* 10 (3), 387–394.
- Obregón, N., Puente, C.E., Sivakumar, B., 2002b. A deterministic geometric representation of temporal rainfall. Sensitivity analysis for a storm in Boston. *J. Hydrol.* 269 (3–4), 224–235.
- Olsson, J., 1998. Evaluation of a scaling cascade model for temporal rainfall disaggregation. *Hydrol. Earth Syst. Sci.* 2 (1), 19–30.
- Olsson, J., Berndtsson, R., 1998. Temporal rainfall disaggregation based on scaling properties. *Water Sci. Technol.* 37 (11), 73–79.
- Pattison, A., 1965. Synthesis of hourly rainfall data. *Water Resour. Res.* 1 (4), 489–498.
- Prairie, J., Rajagopalan, B., Lall, U., Fulp, T., 2007. A stochastic nonparametric technique for space-time disaggregation of streamflows. *Water Resour. Res.* 43 (3). <https://doi.org/10.1029/2005WR004721>.
- Puente, C.E., 1996. A new approach to hydrologic modelling: derived distribution revisited. *J. Hydrol.* 187, 65–80.
- Puente, C.E., 2004. A universe of projections: may Plato be right? *Chaos Soliton Fractals* 19, 241–253.
- Puente, C.E., Obregón, N., 1996. A deterministic representation of temporal rainfall: results for a storm in Boston. *Water Resour. Res.* 32 (9), 2825–2839.
- Puente, C.E., Sivakumar, B., 2007. Modeling hydrologic complexity: a case for geometric determinism. *Hydrol. Earth Syst. Sci.* 11, 721–724.
- Puente, C.E., Robayo, O., Díaz, M.C., Sivakumar, B., 2001a. A fractal–multifractal approach to groundwater contamination. 1. Modeling conservative tracers at the Borden site. *Stoch. Environ. Res. Risk Assess.* 15 (5), 357–371.
- Puente, C.E., Robayo, O., Sivakumar, B., 2001b. A fractal–multifractal approach to groundwater contamination. 2. Predicting conservative tracers at the Borden site. *Stoch. Environ. Res. Risk Assess.* 5 (5), 372–383.
- Puente, C.E., Maskey, M.L., Sivakumar, B., 2018. Studying the complexity of rainfall in time and space via a fractal geometric method. In: Tsonis, A.A. (Ed.), *Advances in Nonlinear Geosciences*. Springer, Cham (in press).
- Salas, J.D., Delleur, J.W., Yevjevich, V., Lane, W.L., 1995. *Applied Modeling of Hydrologic Time Series*. Water Resour. Publ., Littleton, Colorado.
- Schertzer, D., Tchiguirinskaia, I., Lovejoy, S., Hubert, P., Bendjoudi, H., Larchevêque, M., 2002. Which chaos in the rainfall-runoff process. *Hydrol. Sci.* 47 (1), 139–158.
- Sivakumar, B., 2001. Rainfall dynamics at different temporal scales: a chaotic perspective. *Hydrol. Earth Syst. Sci. Discuss.* 5 (4), 645–652.
- Sivakumar, B., 2017. *Chaos in Hydrology: Bridging Determinism and Stochasticity*. Springer Science + Business Media, Dordrecht.
- Sivakumar, B., Sorooshian, S., Gupta, V.J., Gao, X., 2001. A chaotic approach to rainfall disaggregation. *Water Resour. Res.* 37, 61–72.
- Sivakumar, B., Berndtsson, R., Olsson, J., Jinno, K., 2002. Reply to ‘which chaos in the rainfall-runoff process?’ By Schertzer et al. *Hydrol. Sci. J.* 47 (1), 149–158.
- Sivakumar, B., Wallender, W.W., Puente, C.E., Islam, M.N., 2004. Streamflow disaggregation: a nonlinear deterministic approach. *Nonlinear Processes Geophys.* 11, 383–392.
- Stedinger, J.R., Vogel, R.M., 1984. Disaggregation procedures for generating serially correlated flow vectors. *Water Resour. Res.* 20 (1), 47–56.
- Tao, P.C., Delleur, J.W., 1976. Multistation multiyear synthesis of hydrologic time series by disaggregation. *Water Resour. Res.* 12 (6), 1303–1312.
- Tessier, Y., Lovejoy, S., Schertzer, D., 1993. Universal multifractals: theory and observations for rain and clouds. *J. Appl. Meteorol.* 32, 223–250.
- Todini, E., 1980. The Preservation of skewness in linear disaggregation schemes. *J. Hydrol.* 47, 199–214.
- Valencia, D., Schaake, J.C., 1972. A disaggregation model for time series analysis and synthesis. *Mass Inst. Technol., Hydrodyn. Lab. no. 149*.
- Valencia, D., Schaake, J.C., 1973. Disaggregation processes in stochastic hydrology. *Water Resour. Res.* 9 (3), 580–585.
- Zarris, D., Koutsoyiannis, D., Karavokiros, G., 1998. A simple stochastic rainfall disaggregation scheme for urban drainage modelling. In: *Fourth Int. Conf. on Developments in Urban Drainage Modelling*. London, pp. 85–92.